Progress In Electromagnetics Research, Vol. 153, 23–32, 2015

Design and Analysis of a New Axial-Field Magnetic Variable Gear Using Pole-Changing Permanent Magnets

Mu Chen*, Kwok-Tong Chau, Christopher H. T. Lee, and Chunhua Liu

Abstract—This paper presents a new non-rare-earth axial-field magnetic variable gear (MVG). By real-time changing the numbers of permanent magnet (PM) pole-pairs in the input and output rotors, the gear ratio becomes controllable. The key is to propose a new stationary ring integrated with magnetizing windings in such a way that various PM pieces can be independently magnetized to form different pole-pair numbers. After introducing the unique features of the non-rare-earth PM material aluminum-nickel-cobalt (AlNiCo), the proposed topology and design principle are discussed. By using finite element analysis, the electromagnetic performances of the proposed MVG under different gear ratios are analyzed. In particular, the corresponding torque transmission capability is assessed, and the influence caused by the introduction of the magnetizing windings is discussed. Hence, the validity of the proposed MVG can be verified.

1. INTRODUCTION

There are considerable concerns on the development of electric vehicles and wind turbines due to the accelerating demands on green energy and environmental protection [1, 2]. In these applications, the mechanical gearbox plays a vital role for power transmission. Hence, the torque or speed can be properly amplified to fulfill various load conditions. However, the mechanical gearbox inevitably suffers from the drawbacks of contact friction, gear noise and need of regular maintenance [3, 4].

Based on permanent magnet (PM) material, magnetic gears are recognized as one of the most promising candidates to compete with mechanical gears because they offer the merits of noise free, contactless operation and maintenance free [5, 6]. In particular, the coaxial magnetic gear as shown in Figure 1(a) utilizes the principle of magnetic field modulation to realize torque transmission, hence achieving comparable torque density as that of the mechanical gear [7]. Consequently, many types of magnetic gears are derived from the principle of magnetic field modulation. As shown in Figure 1(b), the magnetic gear adopts tangentially magnetized PMs to provide the merits of flux concentration and high mechanical integrity [8]. Then in order to reduce the cost of PM material, the interior-magnet outer-rotor concentric magnetic gear is developed as depicted in Figure 1(c) [9]. Meanwhile, as shown in Figure 1(d), the Halbach magnetic gear incorporates the Halbach PM array to reduce the torque ripple [10].

Since most magnetic gears can only offer a fixed gear ratio, they cannot directly replace the mechanical gearboxes for electric vehicle or wind turbine applications. Thus, some researchers propose the double-rotor machine to perform the concept of electronic-continuously variable transmission [11, 12]. Unfortunately the corresponding slip rings and carbon brushes need regular maintenance, which deteriorates the reliability of the whole system. Consequently the concept of coaxial magnetic variable gear (MVG) is proposed which can offer multiple gear ratios [13]. On the other hand, it has been

Received 27 July 2014, Accepted 29 September 2015, Scheduled 13 October 2015

* Corresponding author: Mu Chen (muchen@eee.hku.hk).

The authors are with the Department of Electrical and Electronic Engineering, The University of Hong Kong, Pokfulam, Hong Kong, China.

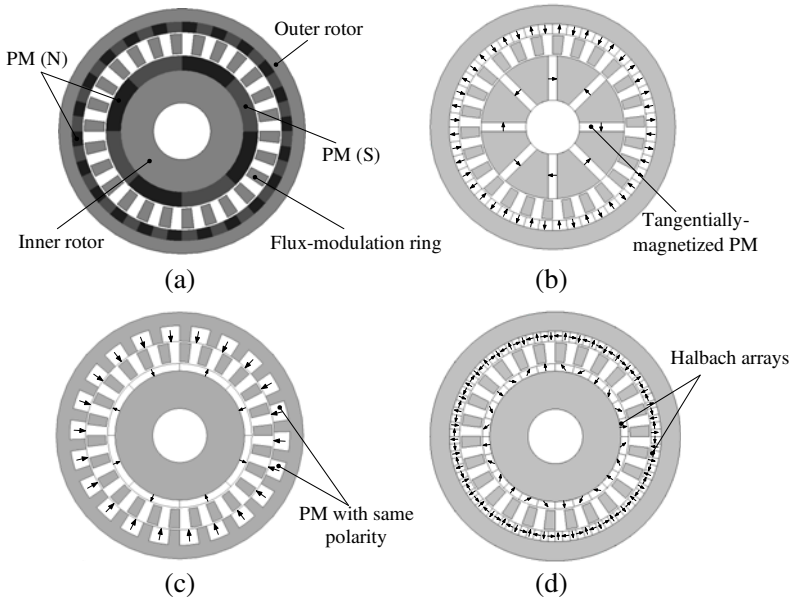

Figure 1. Different magnetic gears: (a) coaxial magnetic gear; (b) magnetic gear with tangentially-magnetized PMs; (c) interior-magnet outer-rotor concentric magnetic gear; (d) Halbach magnetic gear.

identified that the magnetic gears can offer various morphologies such as the axial-field morphology [14] and linear-field morphology [15]. In particular, the axial-field magnetic gear takes the definite advantages of higher torque density and higher power density than its radial-field counterpart because the axial-field morphology can offer larger effective areas than the radial-field one for torque production [16].

This paper aims to extend the concept of coaxial MVG to the axial-field counterpart, hence achieving high torque density with changeable gear ratios. The key is to positively utilize the major drawback of the non-rare-earth PM material aluminum-nickel-cobalt (AlNiCo), namely the low coercivity, to create the capability of changeable gear ratios. Firstly, the development of non-rare-earth PM AlNiCo will be presented. Then, the configuration and design principle of the proposed MVG will be described. By using finite element analysis, the electromagnetic performances of the proposed axial-field MVG under different gear ratios will be simulated and evaluated. Meanwhile, the influence caused by the introduction of the magnetizing winding will be discussed.

2. DEVELOPMENT OF POLE-CHANGING PMS

Figure 2 briefly depicts the development of PM materials [17]. Among them, the ferrite, AlNiCo, samarium-cobalt (SmCo) and neodymium-iron-boron (NdFeB) are four main types of PM materials. Nowadays the NdFeB and SmCo PMs are widely adopted because of their high energy product, high remanence and high coercivity. However, they desire rare-earth elements which are very expensive and suffer from shortage of supply. Table 1 quantitatively summarizes the natural magnetic properties of these four types of PMs, where B_r is remanence, H_c is the coercivity, $BH_{\max}$ is the maximum energy product and T_c is Curie temperature.

The AlNiCo is a non-rare-earth PM, which is composed of aluminum nickel cobalt, a small amount of copper and a balance of iron. It is a potential candidate to compete with the rare-earth PMs for magnetic gear application because it can offer the merits of high remanence, high Curie temperature and very low cost [18, 19]. Although the AlNiCo PM suffers from low coercivity which is the capability to withstand demagnetization, it can be positively utilized to perform controllable magnetization such as for memory machines.

The first memory machine was a pole-alterable PM machine [20, 21]. It consists of the stator wound with armature windings and the rotor embedded with AlNiCo PMs. The key of this machine is that it employs the d-axis component of the armature current to magnetize the AlNiCo PMs to various levels of

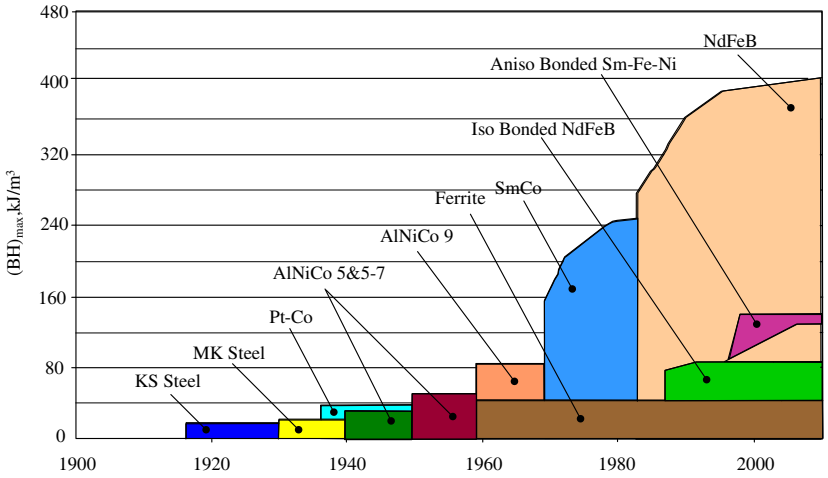

Figure 2. Development of PM materials.

Table 1. Parameters of commonly used PMs.

PM	B_r (T)	H_c (kA/m)	$BH_{\max}$ (kJ/m^3)	T_c (°C)
NdFeB	1.0–1.4	750–2000	200–400	310–400
SmCo	0.8–1.2	600–2000	150–240	720
AlNiCo	0.6–1.35	38–140	10–88	700-860
Ferrite	0.2–0.4	120–300	10–40	450

magnetization, hence achieving different magnitudes of airgap flux density or different numbers of PM pole-pairs. Since the magnetizing current is deduced from the AC armature current, it is so-called the AC-excited memory machine. On the other hand, by incorporating a small DC magnetizing winding into the stator-PM machine to online magnetize the AlNiCo PMs, the DC-excited memory machine is also derived [22, 23]. The DC-excited memory machine takes the advantages of higher robustness and better controllability than the AC-excited counterpart.

In this paper, the concept of DC-excited memory machine is extended to the magnetic gear. Namely, the numbers of PM pole-pairs in the input and output rotors are online changed by properly magnetizing relevant PM pieces, hence changing the gear ratio of the magnetic gear. Differing from the previous DC-excited memory machine design, the numbers of PM pole-pairs are realized by magnetizing the PM pieces in both the input and output rotors simultaneously.

3. PROPOSED AXIAL-FIELD MVG

In order to fully retain the advantages of axial-field magnetic gears while providing the unique feature of variable-speed gearing, the idea of axial-field MVG is born. Figure 3 shows the topology of the proposed axial-field MVG which consists of the input rotor mounted with axially magnetized PM pieces, the stationary ferromagnetic modulation ring wound with DC magnetizing windings and the output rotor mounted with axially magnetized PM pieces. The key is to artfully embed the double-layer DC magnetizing windings into the modulation ring in such a way that the capability of gear-ratio changing can be obtained. When the input rotor operates at a higher speed with a smaller number of PM pole-pairs and the output rotor runs at a lower speed with a larger number of PM pole-pairs, it realizes the torque amplification. On the contrary, when the input rotor adopts a larger PM pole-pair number and the output rotor uses a smaller PM pole-pair number, it realizes the speed amplification. This feature is actually widely used for variable-speed gearing in automobiles but handled by a complicated mechanical gearbox. Table 2 lists some key parameters of the proposed axial-field MVG.

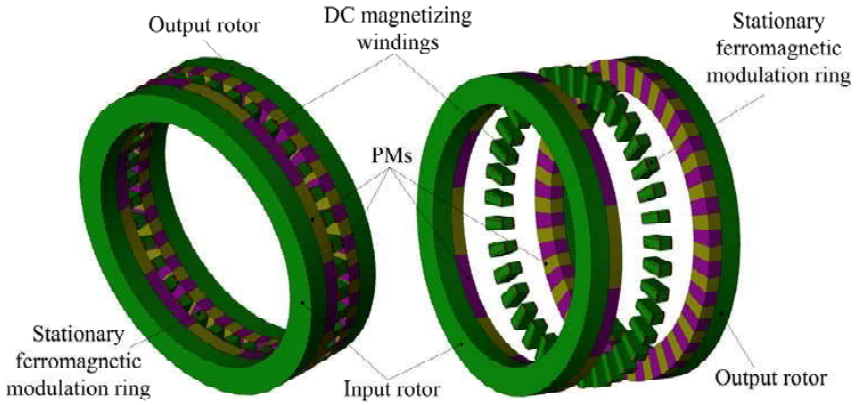

Figure 3. Configuration of proposed axial-field MVG.

Table 2. Parameters of the proposed axial-field MVG.

Item	Axial-field MVG
No. of PM pole-pairs in input rotor	6, 7, 8, 9, 28, 29, 30, 31
No. of PM pole-pairs in output rotor	31, 30, 29, 28, 9, 8, 7, 6
No. of ferromagnetic segments in stationary ring	37
Active outer diameter	220 mm
Axial length of input rotor	25 mm
Axial length of output rotor	25 mm
Axial length of PMs	10 mm
No. of DC magnetizing winding turns for input rotor	100
No. of DC magnetizing winding turns for output rotor	100

Firstly, in order to inherit the advantage of real-time changeable magnetization of PMs from the memory machine, the non-rare-earth PM material AlNiCo is adopted in the proposed axial-field MVG. Although the rare-earth PM based magnetic gears generally have better torque transmission than the non-rare-earth based magnetic gears, the non-rare-earth PM material AlNiCo can offer better cost-effectiveness than the rare-earth PM material [19]. Also, the accident demagnetization of AlNiCo is invalid for the proposed axial-field MVG because of the absence of armature windings. Particularly, the high Curie temperature of AlNiCo makes it preferable for operating in harsh environment.

By properly designing the number of iron segments in the modulation ring, namely 37, the proposed axial-field MVG can offer 8 discrete sets of gear ratios, namely from 0.19 to 5.16. In order to realize the ability of changeable PM pole-pairs, the double-layer DC magnetizing windings are incorporated into the modulation ring. As shown in Figure 4, the double-layer DC magnetizing windings can be easily inserted into the modulation ring since the windings just need to carry a temporary current for magnetization of PM pieces in the input and output rotors. When the gear-ratio changing mode is activated, namely the desired gear ratio is different from the existing gear ratio the double-layer DC magnetizing windings are injected with proper DC currents to magnetize the desired PM pieces. The process of magnetization of PM pieces in the two rotors are activated simultaneously to realize the desired numbers of pole-pairs so that the gear-ratio changing can be achieved within a short period, typically a few milliseconds. For the normal operation mode, the double-layer magnetizing windings are open-circuited so that they will not induce any circulating current to cause an adverse effect on the torque transmission. Nevertheless, the presence of magnetizing windings inevitably reduces the output torque and torque capability because of the reduction of effective area of the ferromagnetic material in the modulation ring.

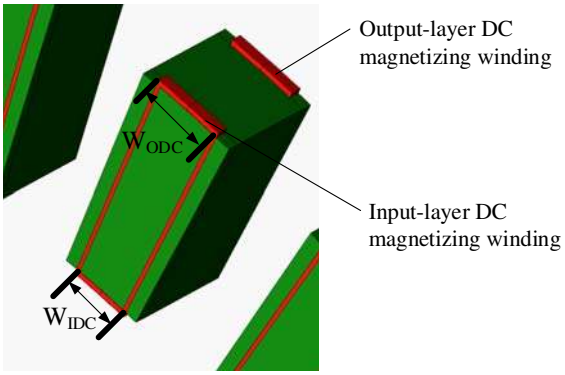

Figure 4. Stationary ferromagnetic modulation ring with DC magnetizing windings.

The design parameters of the proposed axial-field MVG are governed by:

$$\begin{cases} N_s = N_i + N_o, \quad G_r = \frac{N_o}{N_i} \\ M_1 = (\ m_{11} \quad m_{12} \quad m_{1k} \quad \ldots \quad m_{1(N_s-1)}\ ) \\ m_{1k} = [N_s - k, k] \quad k = 1, 2, 3, \ldots, (N_s - 1) \\ N_{mi} = N_{mo} = 2n[\underbrace{\ m_{1j}, \quad \ldots, \quad m_{1y}\ }_{selected\ gear\ ratios}] \\ N_{ow} = N_{iw} = N_s, \quad T_s + T_i + T_o = 0 \\ n = 1, 2, 3, \ldots \quad j, y = 1, 2, \ldots, (N_s - 1) \end{cases} \tag{1}$$

where N_s is the number of ferromagnetic segments in the stationary ring, N_i is the number of PM pole-pairs in the input rotor N_o is the number of PM pole-pairs in the output rotor, G_r is the gear ratio, M_1 is the least number of PM pieces, m_{1k} is the least number of PM pieces of one possible gear ratio, N_{mi} is the number of PM pieces in the input rotor, N_{mo} is the number of PM pieces in the output rotor, N_{ow} is the number of turns of the output-layer magnetizing winding, and N_{ow} is the number of turns of the input-layer magnetizing winding, and T_s, T_i and T_o are the electromagnetic torques developed at the stationary ring, input rotor and output rotor, respectively. Also, considering the practicability of the proposed axial-field MVG, the active widths of DC magnetizing windings are determined by:

$$\begin{cases} W_{ODC} = \dfrac{\pi R_{os}}{nN_o} < \dfrac{\pi R_{os}}{N_s}, \quad W_{IDC} = \dfrac{\pi R_{is}}{nN_i} < \dfrac{\pi R_{is}}{N_s} \\ m = 1, 2, 3, \ldots, \quad n = 1, 2, 3, \ldots \end{cases} \tag{2}$$

where W_{ODC} is the upper width of the magnetizing winding, W_{IDC} is the lower width of the magnetizing winding, R_{os} is the active outer radius, and R_{is} is the active inner radius of the proposed MVG. Meanwhile, W_{ODC} and W_{IDC} should be as large as possible.

4. ELECTROMAGNETIC PERFORMANCE ANALYSIS

By using the finite element analysis software JMAG, the electromagnetic performances of the proposed axial-field MVG under different gear ratios are simulated. By properly changing the PM pole-pair numbers on the input rotor and output rotor, the gear ratio can be flexibly varied to fulfill different output requirements.

The process of gear-ratio changing starts when the existing gear ratio differs from the desired gear ratio. Since the gear ratio is governed by the numbers of PM pole-pairs in the output and input rotors, the relevant PM pieces that need changes in magnetic polarity are determined accordingly. In order to change the magnetic polarity of relevant PM pieces, the magnetizing windings located in the stationary ring are properly energized. Hence, the magnetizing current is used to effectuate the gear-ratio changing. Figure 5 illustrates how to change the magnetic polarity of one pair of PM pieces. It can be observed that initially the direction of magnetic flux in both the PM pieces 1 and 2 is from the right to the

left. After injecting the DC current of 5 A into the magnetizing windings, the corresponding direction is reversed, namely from the left to the right. Since the two PM pieces can be simultaneously magnetized, the overall process is very effective. It should be noted that the magnetizing current should be applied at the instant that the PM piece 1 aligns with the PM piece 2. Such alignment can be ensured by simply using two position sensors coupled with the two rotors.

Moreover, in order to ensure that the magnetizing current is high enough to perform the desired gear-ratio changing, the change of the direction of magnetization of relevant PM pieces can be judged by the flux line during the simulation. For practical application, the magnetizing current is generally 20% higher than the simulation value to guarantee the success of gear-ratio changing.

According to the operation principle, the parameter N_s is selected as 37 so that N_o can be set as 6, 7, 8, 9, 28, 29, 30 and 31 while the N_i can be set as 31, 30, 29, 28, 9, 8, 7 and 6 respectively. Hence,

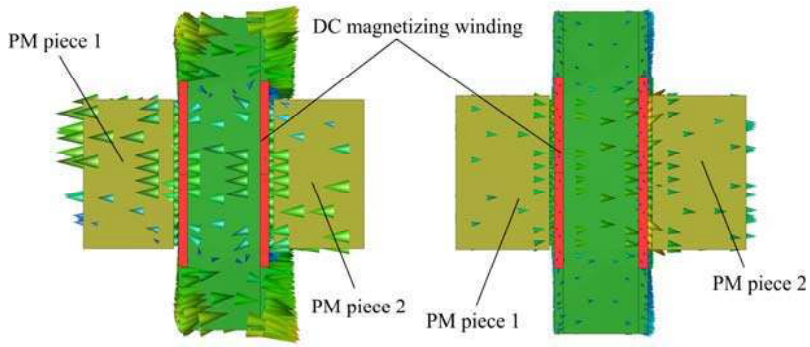

Figure 5. Gear-ratio-changing process of PM pieces: (a) initial magnetization direction; (b) new magnetization direction.

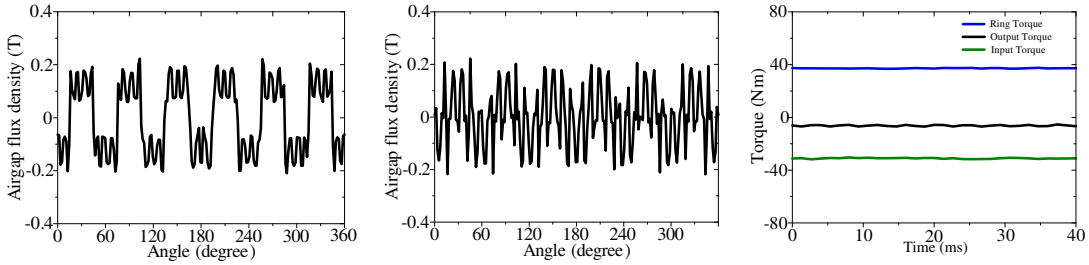

Figure 6. Electromagnetic performances under $G_r = 6/31$: (a) airgap adjacent to output rotor; (b) airgap adjacent to input rotor; (c) torque transmission.

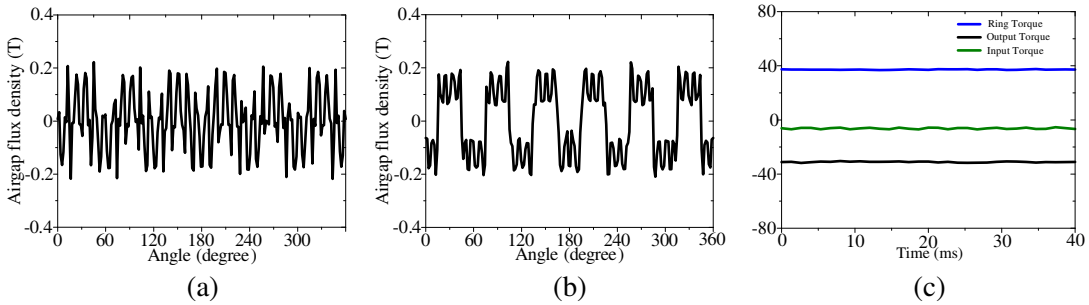

Figure 7. Electromagnetic performances under $G_r = 31/6$: (a) airgap adjacent to output rotor; (b) airgap adjacent to input rotor; (c) torque transmission.

8 discrete gear ratios $G_r = 6/31$, $G_r = 7/30$, $G_r = 8/29$, $G_r = 9/28$, $G_r = 28/9$, $G_r = 29/8$, $G_r = 30/7$ and $G_r = 31/6$ are resulted.

The waveforms of airgap flux density and steady-state torque under 8 sets of gear ratios ($G_r = 6/31$, $G_r = 7/30$, $G_r = 8/29$, $G_r = 9/28$, $G_r = 28/9$, $G_r = 29/8$, $G_r = 30/7$ and $G_r = 31/6$) are simulated. Among them, the waveforms under two typical cases, namely $G_r = 6/31$ for torque reduction (speed amplification) and $G_r = 31/6$ for torque amplification (speed reduction) are shown in Figures 6 and 7, respectively. From the airgap flux density waveforms in Figure 6, it confirms that the number of pole-pairs in the output airgap is 6 and the number of pole-pairs in the input airgap is 31, which well agrees with the gear ratio of $G_r = 6/31$. From the torque waveforms in Figure 6, it can be observed that the steady-state torques at the output rotor and input rotor are 6.12 Nm and 31.05 Nm, respectively, which are in accordance with the gear ratio. Also, it can be observed that the torque exerted at the stationary ring is 37.3 Nm which equals the sum of the input steady-state torque and the output steady-state torque, validating the theoretical analysis. Meanwhile, the airgap flux density waveforms and torque waveforms shown in Figure 7 well agree with the gear ratio of $G_r = 31/6$ and the theoretical analysis. Consequently, all steady-state torques under 8 sets of gear ratios are summarized in Table 3. It can be observed that the relationship between the torques at the input rotor and output rotor well agree with their gear ratios.

Table 3. Steady-state torque performance of proposed MVG.

Gear ratio	Output torque	Input torque	Ring torque
6/31	6.12 Nm	31.05 Nm	37.3 Nm
7/30	7.5 Nm	31.95 Nm	39.8 Nm
8/29	8.85 Nm	32.4 Nm	40.98 Nm
9/28	10.12 Nm	30.87 Nm	40.82 Nm
28/9	30.87 Nm	10.12 Nm	40.82 Nm
29/8	32.4 Nm	8.85 Nm	40.98 Nm
30/7	31.95 Nm	7.5 Nm	39.8 Nm
31/6	31.05 Nm	6.12 Nm	37.3 Nm

In addition, the torque transmission capability of the proposed axial-field MVG can be obtained by holding the output rotor while rotating the input rotor. Table 4 summarizes the torque transmission capabilities under 8 gear ratios. It can be observed that when $G_r = 6/31$ the maximum torque exerted on the output rotor is 6.23 Nm while the maximum input torque is 31.62 Nm which further confirms that the torque transmission capability well agrees with the gear ratio. Obviously, the gear ratios $G_r = 6/31$, $G_r = 7/30$, $G_r = 8/29$ and $G_r = 9/28$ are used for those applications desiring speed amplification. Meanwhile, the gear ratios $G_r = 28/9$, $G_r = 29/8$, $G_r = 30/7$ and $G_r = 31/6$ are adopted for those applications desiring torque amplification. With these 8 gear ratios, the proposed axial-field MVG becomes very useful for those applications with wide speed and torque ranges. Particularly, the torque density of the proposed MVG can achieve 14.38 $\mathrm{kN/m^3}$ which is very acceptable.

Furthermore, a comparative study of the proposed MVG with and without including the magnetizing windings is conducted. Table 3 and Table 4 summarize the electromagnetic performances of the proposed MVG which has included the magnetizing windings while Table 5 presents the torque performances of the proposed MVG if the magnetizing windings are omitted. It should be noted that the magnetizing windings are mandatory to provide the capability of gear-ratio changing, whereas the analysis in the absence of magnetizing windings aims to show the drawback accompanied with gear-ratio changing. As shown in Table 3, the torque developed at the output rotor is 6.12 Nm under $G_r = 6/31$. As listed in Table 5, if there is no magnetizing winding in the stationary ring, the corresponding torque will be 6.95 Nm, which indicates that the inclusion of magnetizing windings has caused 12% reduction of output torque. In addition, if the magnetizing windings are absent, the maximum torque developed at the input rotor under $G_r = 6/31$ will be 35.79 Nm as listed in Table 5. Obviously, in the presence magnetizing windings, the corresponding torque is 31.62 Nm as listed in Table 4, which also indicates that there is 11.7% reduction of torque capability due to the introduction of magnetizing windings. It

Table 4. Torque transmission capability of proposed MVG.

Gear ratio	Output torque	Input torque
6/31	6.23Nm	31.62 Nm
7/30	7.61 Nm	33.2 Nm
8/29	8.9 Nm	32.8 Nm
9/28	9.78 Nm	31.1 Nm
28/9	31.1 Nm	9.78 Nm
29/8	32.8 Nm	8.9 Nm
30/7	33.2 Nm	7.61 Nm
31/6	31.62 Nm	6.23Nm

Table 5. Torque performances of proposed MVG without considering magnetizing windings.

Gear ratio	Output torque (Reduction)	Torque capability (Reduction)
6/31	6.95 Nm (12%)	35.79 Nm (11.7%)
7/30	8.3 Nm (9.7%)	36.52 Nm (9.1%)
8/29	9.86 Nm (10.2%)	36.64 Nm (10.5%)
9/28	11.18 Nm (9.5%)	34.14 Nm (8.9%)
28/9	34.15 Nm (9.6%)	34.14 Nm (8.9%)
29/8	36.03 Nm (10%)	36.64 Nm (10.5%)
30/7	35.46 Nm (9.9%)	36.52 Nm (9.1%)
31/6	35.2 Nm (11.8%)	35.79 Nm (11.7%)

is actually the price that the MVG needs to pay for the flexibility of gear-ratio changing which is very desirable for some industrial applications.

It should be noted that the reductions of output torque and torque capability due to the introduction of magnetizing windings are inevitable because the effective area of the ferromagnetic material in the modulation ring is reduced in order to accommodate those copper windings. Thus, the flux modulation is adversely affected and the torque reduction is resulted. Nevertheless, the ferromagnetic modulation ring does not incur significant power loss because the copper loss occurs only during the process of gear-ratio changing which is only a short duration, and the iron loss is negligible as the operating frequency is normally less than 100 Hz.

5. CONCLUSION

This paper has presented a new axial-field MVG which incorporates the concept of axial-field magnetic gears and the concept of memory machines. The key is to online changing the numbers of PM pole-pairs in the input rotor and output rotor, hence achieving changeable gear ratios. The simulation results confirm that the proposed MVG can offer 8 discrete gear ratios, which will be very useful for those applications demanding a wide range of speeds and torques such as electric vehicles and wind turbines. Although the introduction of magnetizing windings for attaining the capability of gear-ratio changing inevitably degrades the torque transmission by at most 12%, the proposed magnetic gear can provide the unique feature of changeable gear ratios while achieving the torque density of 14.38 kN/m^3.

ACKNOWLEDGMENT

This work was supported by a grant (Project No. HKU710612E) from the Hong Kong Research Grants Council, Hong Kong Special Administrative Region, China.

REFERENCES

1. Chau, K. T. and C. C. Chan, "Emerging energy-efficient technologies for hybrid electric vehicles," *Proceedings of IEEE*, Vol. 95, No. 4, 821–835, 2007.
2. Chau, K.-T., W. Li, and C. H. T. Lee, "Challenges and opportunities of electric machines for renewable energy," *Progress In Electromagnetics Research B*, Vol. 42, 45–74, 2012.
3. Nakamura, K., M. Fukuoka, and O. Ichinokura, "Performance improvement of magnetic gear and efficiency comparison with conventional mechanical gear," *Journal of Applied Physics*, Vol. 115, 17A314, 2014.
4. Jian, L., K. T. Chau, Y. Gong, J. Z. Jiang, C. Yu, and W. Li, "Comparison of coaxial magnetic gears with different topologies," *IEEE Transactions on Magnetics*, Vol. 45, No. 10, 4526–4529, 2009.
5. Jian, L. and K.-T. Chau, "Analytical calculation of magnetic field distribution in coaxial magnetic gears," *Progress In Electromagnetics Research*, Vol. 92, 1–16, 2009.
6. Li, X., K.-T. Chau, M. Cheng, and W. Hua, "Comparison of magnetic-geared permanent-magnet machines," *Progress In Electromagnetics Research*, Vol. 133, 177–198, 2013.
7. Atallah, K. and D. Howe, "A novel high-performance magnetic gear," *IEEE Transactions on Magnetics*, Vol. 37, No. 4, 2844–2846, 2001.
8. Rasmussen, P. O., T. O. Andersen, F. T. Jorgensen, and O. Nielsen, "Development of a high-performance magnetic gear," *IEEE Transactions on Industry Applications*, Vol. 41, No. 3, 764–770, 2005.
9. Liu, X., K. T. Chau, J. Z. Jiang, and C. Yu, "Design and analysis of interior-magnet outer-rotor concentric magnetic gears," *Journal of Applied Physics*, Vol. 105, 07F101, 2009.
10. Jian, L. and K. T. Chau, "A coaxial magnetic gear with Halbach permanent magnet arrays," *IEEE Transactions on Energy Conversion*, Vol. 25, No. 2, 319–328, 2010.
11. Chau, K. T., *Electric Vehicle Machines and Drives — Design, Analysis and Application*, Wiley-IEEE Press, 2015.
12. Sun, X., M. Cheng, W. Hua, and L. Xu, "Optimal design of double-layer permanent magnet dual mechanical port machine for wind power application," *IEEE Transactions on Magnetics*, Vol. 45, No. 10, 4613–4616, 2009.
13. Chen, M., K. T. Chau, W. Li, C. Liu, and C. Qiu, "Design and analysis of a new magnetic gear with multiple gear ratios," *IEEE Transactions on Applied Superconductivity*, Vol. 24, No. 3, 0501904, 2014.
14. Mezani, S., K. Atallah, and D. Howe, "A high-performance axial-field magnetic gear," *Journal of Applied Physics*, Vol. 99, 08R303, 2006.
15. Li, W. and K.-T. Chau, "Analytical field calculation for linear tubular magnetic gears using equivalent anisotropic magnetic permeability," *Progress In Electromagnetics Research*, Vol. 127, 155–171, 2012.
16. Lee, C. H. T., K. T. Chau, C. Liu, T. W. Ching, and F. Li, "A high-torque magnetless axial-flux doubly-salient machine for in-wheel direct drive applications," *IEEE Transactions on Magnetics*, Vol. 50, No. 11, 8202405, 2014.
17. Kramer, M. J., R. W. McCallum, I. A. Anderson, and S. Constantinides, "Prospects for non-rare-earth permanent magnets for traction motors and generators," *Journal of the Minerals, Metals and Materials Society*, Vol. 64, No. 7, 752–763, 2012.
18. Chen M., K. T. Chau, W. Li, and C. Liu, "Development of non-rare-earth magnetic gears for electric vehicles," *Journal of Asian Electric Vehicles*, Vol. 10, No. 2, 1607–1613, 2012.
19. Chen, M., K. T. Chau, W. Li, and C. Liu, "Cost-effectiveness comparison of coaxial magnetic gears with different magnet materials," *IEEE Transactions on Magnetics*, Vol. 50, No. 2, 7020304, 2014.
20. Ostovic, V., "Pole-changing permanent-magnet machines," *IEEE Transactions on Industry Applications*, Vol. 38, No. 6, 1493–1499, 2002.
21. Ostovic, V., "Memory motors," *IEEE Industry Applications Magazine*, Vol. 9, No. 1, 52–61, 2003.

22. Yu, C., K. T. Chau, and J. Z. Jiang, "A flux-mnemonic permanent magnet brushless machine for wind power generation," *Journal of Applied Physics*, Vol. 105, No. 7, 07F114, 2009.
23. Yu, C., and K. T. Chau, "Design, analysis and control of DC-excited memory motors," *IEEE Transactions on Energy Conversion*, Vol. 26, No. 2, 479–489, 2011.